doi:10.3788/gzxb20154401.0112001

基于功率谱的大口径望远镜面型评价

安其昌[1],张景旭[1],杨飞[1],张丽敏[1],刘祥意[1,2]
(1 中国科学院 长春光学精密机械与物理研究所,长春 130033)
(2 中国科学院 研究生院,北京 100039)

摘　要:为了更好地评价与研究受视宁影响的观测系统,引入了基于功率谱的分析方法.使用不同截止频率以及衰减系数的卡曼谱来反演系统的中高频误差,同时使用 Zernike 多项式来表征系统低阶起伏,结合这两种误差,得到了系统误差的数值模型.最后,通过分析实际波前叠加数值模拟大气扰动前后的功率谱,验证了本方法评价受视宁影响的大口径系统的可行性.

关键词:功率谱 ;波前误差; 卡曼模型;大气扰动;大口径望远镜
中图分类号:TH751　　**文献标识码**:A　　**文章编号**:1004-4213(2015)01-0112001-5

Large Aperture Telescope Mirror Figure Evaluation with Power Spectral Density

AN Qi-chang[1], ZHANG Jing-xu[1], YANG Fei[1], ZHANG li-min[1], LIU Xiang-yi[1,2]
(1 *Changchun Institute of Optics, Fine Mechanics and Physics, Chinese Academy of Sciences, Changchun* 130033, *China*)
(2 *Graduate University of Chinese Academy of Sciences, Beijing* 100039, *China*)

Abstract: The power spectral density was investigated to analyze the seeing-limited performance of large telescope. The Karman spectral with different frequency knees and the Power Spectral Density (PSD) slope were used to simulate the atmosphere turbulence. And the Zernike polynomials was used to analyze the low order deviations. Combining the two kinds of deviation, the numeral modal was built to simulate the system. Lastly, by analyzing the PSD of actual sample and the sample combined with the numeral atmosphere turbulence, the separation of the abberations with different sourse was obtained. The results show that the proposed method can specify the performance of the large telescope under limited seeing.

Key words: Power spectral; Wave front error; Karman model; Atmosphere turbulence; Large telescope
OCIS Codes: 120.4640; 120.4610; 120.4800; 120.5050

0 Introduction

Theoptical performance of the large aperture telescope is a major concern for the next generation ground based facilities. For optimizing these performances, the frequency domain metric is placed more and more significance. First and foremost, an adequate metric for charactering large surface figure should possess the frequency domain property. In addition, the metric should be easily received . The large telescopes, such as Thirty Meter Telescope (TMT), have paid more and more attention to the seeing limit. For the TMT, the seeing condition is evaluated by the Slope Root Mean Square (Slope RMS)[1-5].

The mirror surface figure of large telescope is mainly influenced by design, manufacture and metrology, which conld be taken to consideration in the evaluation phase. The RMS of the Wave Front Error (WFE) is a universally accepted metric. However, when it comes to the large telescope case, the RMS is not by itself adequate. When the higher spatial frequency is involved, the WFE may degrade into many types, which may have the same RMS. That means

Foundation item: The National High Technology Research (863)(No. 2012AAXXX1003P)
First author: AN Qi-chang(1988－), male, research assistant, M. S. degree, mainly focuses on large aperture telescope testing. Email: anjj@mail. ustc. edu. cn
Received: Apr. 22, 2014; **Accepted**: Sep. 15, 2014

RMS has not dynamic property, and it is unable to show the aberrations in varied of dimensions[6-7].

Though the Zernike polynomials are good to specify the low spatial frequency components of the wave front, the calculation cost dramatic increases as the order rises. Furthermore, even up to the 100th Zernike polynomial, the spatial frequency resolution is still limited to 13 in both radial and circumferential direction. So, the Zernike polynomials are only proper to character the multiple WFE, with a few low spatial frequency compositions[8-12].

We consequently involve the Power Spectral Density (PSD) to specify the seeing-limited performance of large telescope . It has been originally researched by American national ignition facility in 1990s[13-16]. This metric is directly related to the different spatial frequency distribution. The PSD metric can do the evaluation more efficiently with Fast Fourier Transfer (FFT).

1 Definition

Firstly, suppose a stochastic process $\{X(t), t\in T\}$, at every $t\in T$ for $X(t)$, $E[X(t)]$ and $E[X^2(t)]$ both existing. In this condition, $\{X(t), t\in T\}$ is noted as quadratic process.

Generally, without destruction of the optical surface, the wave front error $\varphi(x)$ can rarely boost to infinite. So the $E[\varphi(x)]$ and $E[\varphi^2(x)]$ always exist. We assume that the aberration is quadratic error. We take its correlation coefficient $R(\varphi(x+r), \varphi(x))$ into condition. It has the following property

$$R^2(\theta(x+r), \theta(x)) = \{E[\theta(x+r)\theta(x)]\}^2 \leqslant E[\theta^2(x+r)]E[\theta^2(x)] < +\infty \quad (1)$$

For ideal wave front error, the direct current composition of the mirror figure should be zero. The stochastic process generated from the data is consequently considered as wide steady process. The power spectral density of this process is noted as

$$S(\omega) = \sum_{-\infty}^{\infty} R(m)\mathrm{e}^{-\mathrm{j}\omega} = \sum_{-\infty}^{\infty} E[x(n)x^*(n+m)]\mathrm{e}^{-\mathrm{j}\omega} \quad (2)$$

Consider two-dimension condition:

$$s(u,v) = \frac{1}{L'L} \times \left| \sum_{m=0}^{L'-1}\sum_{n=0}^{L-1} \omega(m,n) X(m+i'D', n+iD)\mathrm{e}^{-\mathrm{j}(mu+nv)} \right|^2 \quad (3)$$

In the Eq. (3), a welch window is defined as

$$\omega(n,m) = 1 - \left| \frac{\sqrt{m^2+n^2}}{\sqrt{L^2+L'^2}} \right|^{\alpha} \quad (4)$$

where L, L' are the maximum values of n, m, respectively, inside the surface map aperture. A welch window can eliminate both smearing and leakage problem . A parameter of $\alpha = 8$ was found to have a good compromise between them.

The two-dimension PSD defined in Eq. (3) is able to process an overall evaluation. It cannot provide concrete value. We prefer to collapse the result, as what has been done by American National Ignition Facility (NIF), meanwhile in a better method.

Generally, we collapse the Two-Dimension PSD (2D-PSD) in time or frequency domain. For time domain collapse method (just like what has been done by NIF), the accuracy degrades remarkably, when the wave front is not rotating symmetric. For the other one, with the symmetric property of FFT, we can make the collapse more smooth and accuracy.

We do the collapse in the following way

$$\bar{\rho}_i = \frac{1}{N_i}\sum_{N_{i-1}}^{N_i} \rho_l \quad (5)$$

where, $\bar{\rho}_i$ is the average radius

$$\mathrm{PSD}_{1\mathrm{D}} = \frac{1}{N}\sum_{N_{i-1}}^{N_i} \mathrm{PSD}_{2\mathrm{D}}(\rho_l)$$

In the Fig. 1, the wave front of a laser beam is showed. We process the wave front in the way mentioned in this section. Collapse is done fromthe 2D PSD and the result is revealed in Fig. 2.

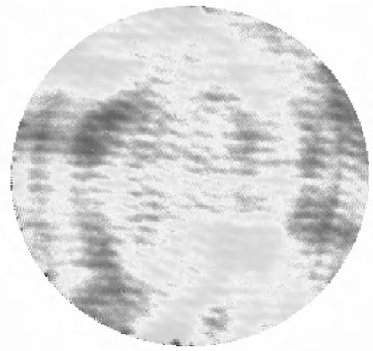

Fig. 1 Wave front of a laser system

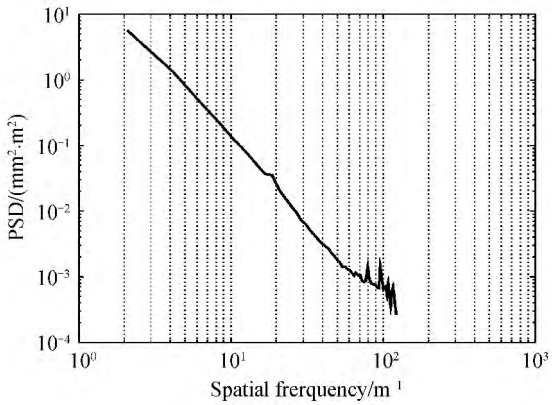

Fig. 2 The 1D PSD achieved by collapse

As seen in Fig. 2, the aberration mainly converges in the mid-high frequency domain and we can evaluate the error separately. The PSD method can evaluate the wave front not only qualitatively but also in ration. The NIF has showed a Not-To-Pass (NTP) curve. If the PSD does not intersect the cure in certain frequency range, the wave front is acceptable.

2 Properties

The WFE always contains two components that the low order aberrations and the high order ones. The Zernike polynomials are the most universal metric to specify the low order error. Here, assume the wave front is composed by two terms of Zernike polynomials

$$\phi = c_i\phi_i + c_j\phi_j \tag{6}$$

After dispersed, it also has similar relationship

$$\Phi(n) = c_i\Phi_i(n) + c_j\Phi_j(n) \tag{7}$$

Then ,we calculate the PSD

$$S(\omega) = \sum_{-\infty}^{\infty} R(m)\mathrm{e}^{-\mathrm{j}\omega} = \sum_{-\infty}^{\infty}\{E[\Phi(n)\Phi^*(n+m)]\} \cdot \mathrm{e}^{-\mathrm{j}\omega} = \sum_{-\infty}^{\infty}\{E[c_i\Phi_i(n)+c_j\Phi_j(n)][c_i\Phi_i(n+m)+c_j\Phi_j(n+m)]^*\}\mathrm{e}^{-\mathrm{j}\omega} = \sum_{-\infty}^{\infty}\{E[c_i\Phi_i(n)c_i\Phi_i^*(n+m)+c_j\Phi_j(n)c_j\Phi_j^*(n+m)+c_i\Phi_i(n)c_j\Phi_j^*(n+m)+c_i\Phi_j(n)c_i\Phi_j^*(n+m)]\}\mathrm{e}^{-\mathrm{j}\omega} \tag{8}$$

For the orthogonal property of the Zernike polynomials, we can achieve

$$S(\omega) = \sum_{-\infty}^{\infty}\{E[c_i\Phi_i(n)c_i\Phi_i^*(n+m)+c_j\Phi_j(n)c_j \cdot \Phi_j^*(n+m)]\}\mathrm{e}^{-\mathrm{j}\omega} = c_i^2R_i(m)+c_j^2R_j(m) \tag{9}$$

For the atmosphere turbulence case, the WFE can be described by the von Karman PSD as

$$\mathrm{PSD}(f) = \frac{\sigma}{(1+(f/f_0)^2)^{\gamma/2}} \tag{10}$$

The von Karman PSD has three parameters as σ, f_0 and γ, which are the amplitude ,the frequency knee and the PSD slope. The amplitude determines the standard deviation of the turbulence wave front. The frequency knee and the PSD slope are employed to achieve the different cut-off frequency.

Varying these parameters, we can obtain different kinds of atmosphere turbulences. This is a very easy-to-use approach to the mid-spatial frequency components of the WFE of an optical system. Using Karman PSD, we can get the atmosphere turbulence wave front , as shown in Fig. 3. In this way , we can consider the seeing-limit condition numerically.

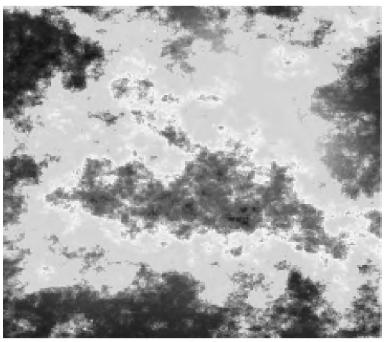

Fig. 3 Karman PSD wave front

The Karman PSD and NIF NTP curve are showed in Fig. 4, we can come to a conclusion that ,for some case, only the error generated by atmosphere is big enough to become a major limit for the performance of large telescope, rather than the manufacture aberration of mirror itself.

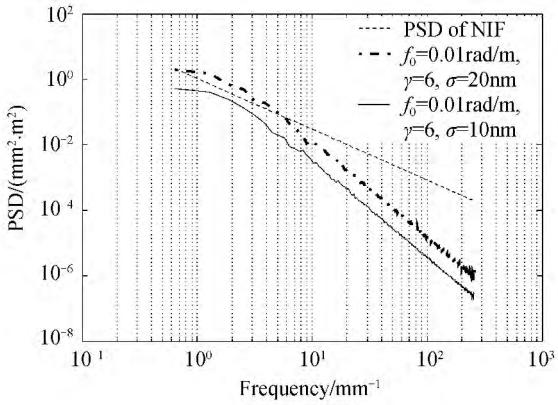

Fig. 4 PSD curve of Karman

3 Verify and analysis

For the low order WFE, we put the method forward to the Zernike polynomials, as shown in Fig. 4. In the figure, the mid and high spatial frequency component is smooth. That means there is no middle frequency roughness in this case. The deviation from perfect mirror surface is only effected by the gravity print though. As is showed in Section 2, we can analysis the PSD of Zernike polynomialsseparately and multiply them . We can also study the residual height map after some terms removed.

On the other hand, if the mirror surface contains mid-spatial frequency error, the according region will raise, as shown in Fig. 5.

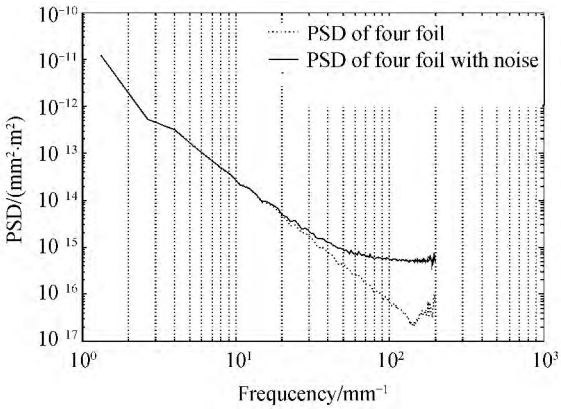

Fig. 5 The PSD of four foil

In most conditions of large telescope testing, the best way to specify the mid-high spatial frequency error of the mirror is given as follows: evaluate the print by the low order Zernike polynomials, after they are removed,the residual component with higher frequency will be analyzed by PSD method, representing the atmosphere turbulence and roughness.

We use the testing result of a 1.23 m reflecting mirror in Changchun Institute of Optics, Fine

Mechanics and Physics, Chinese Academy of Sciences, which is showed in Fig. 6. We can also obtain the atmosphere turbulence in the according aperture by Karman PSD.

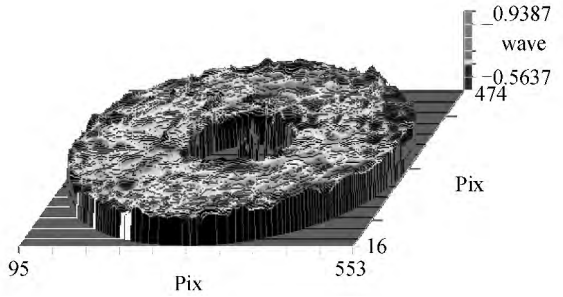

Fig. 6 1.23 m mirror figure

The 1.23 m surface height map, with piston, tip/tilt Zernike items removed, is overlaid by the atmosphere turbulence. We simulate the crosstalk condition of the manufacture roughness and the atmosphere turbulence as shown in Fig. 7.

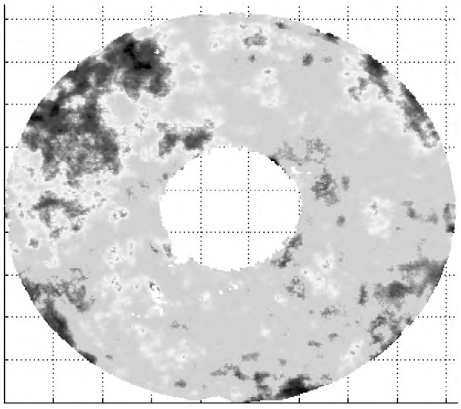

Fig. 7 Coupling wave front error

By the means in Section 2, we plot the PSD of the sample coupling with the Karman PSD of $\sigma=3$ nm, $f_0=0.01$ rad/m, $\gamma=5$ and $\sigma=3$ nm $f_0=0.01$ rad/m, $\gamma=6$, in Fig. 8.

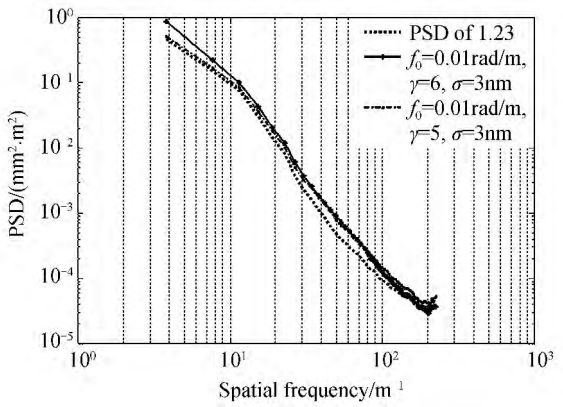

Fig. 8 PSD of 1.23 m mirror

As seen in the figure, We can draw a the conclusion that for the adding of atmosphere turbulence, the PSD curve raises, closer to the NTP . On the other hand, as the PSD slope γ decreases, the middle frequency component increases.

The atmosphere turbulence cannot rise the high spatial frequency part of the PSD curve, because the band widthof the atmosphere turbulence is finite.

For the actual testing and error budget, we can take all the factors into condition, such as atmosphere turbulence, manufacture and metrology error . Additionally, with the NTP curve, we can consider the error quantitatively.

4 Conclusion

For large aperture optical system, the mere consideration for the roughness of the mirror itself is not adequate. The influence of atmosphere, namely seeing, must be placed significant.

Carrying out the calculation of the PSD to estimate the middle and high spatial frequency aberration is an effective method for analyze seeing-limited large telescope. Furthermore, we introduce the collapse method to specify it more briefly and clearly. We expect the reaserch can be halpful for the analysis of optic surface and become a valuable reference for the beginners in this field.

Acknowledgement *The author is very grateful to Dr. ZHAO Hong-chao for providing his valuable suggestion.*

References

[1] ZHANG Wei, LIU Jian-feng, LONG Fu-nian. *et al*. Study on wavefront fitting using Zernike polynomials [J]. *Optic Technique*, 2005, **31**(5): 675-678.

[2] BI Yong, ZHAI Jia, WU Jing-yong, *et al*. One method for mirror surface figure treatment in optical instrument[J]. *Optic Technique*, 2009, **35**(1): 10-17.

[3] WANG Yu-chun, SUN He-yi, TANG Wen-yan, *et al*. Angle subdivision approach algorithm for conicoid profile error evaluation[J]. *Optics and Precision Engineering*, 2014, **22**(6): 1606-1612.

[4] LIN Xu-Dong, LIU Xin-Yue, WANGJian-li, *et al*. Performent of correction capability of 137-element deformable mirror[J]. *Optics Precision Engineering*, 2013, **21**(2): 267-273.

[5] POYNEER L A, van DAM M, VÉRAN J P. Experimental verification of the frozen flow atmosphericturbulence assumption with use of astronomical adaptive optics telemetry [J]. *Journal of the Optical Society of America*, 2009, **26**(4): 833-846.

[6] ZHANG Jin-xu. Overview of structure of technologies of large aperture ground based telescope[J]. *Chinese Optics*, 2012, **5**(4): 327-336.

[7] DIERKING W. RMS slope of exponentially correlated surface roughnessfor radar applications [J]. *IEEE Transactions on Geoscience and Remote Sensing*, 2000, **38**(3): 1451-1454.

[8] ZHELEM R. Specification of optical surface accuracy using the structure function[C]. SPIE, 2011, **8083**: 808310.

[9] SHI Tu, YANG Yong-ying, ZHANG Lei, *et al*. Surface testing methods of aspheric optical elements [J]. *Chinese Optics*, 2014, **7**(1): 26-46.

[10] DONG Yu-hang, CEN Song-yuan. Improving spectrograph

accuracy by bayesian method[J]. *Acta Photonica Sinica*, 2013, **42**(12): 1491-1495.

[11] JIU Jing. Optical system design of the optical multi-function detector[J]. *Acta Photonica Sinica*, 2013, **42**(12): 1507-1513.

[12] WANG Xiao-kun. Fabrication and testing of large aperture off-axis SIC aspheric mirror[J]. *Laser & Optoelectrics Process*, 2011, **49**(1): 011201.

[13] CHEN Bao-gang, MING Ming, LYU Tian-yu. Precise measurement of curvature radius for spherical mirror with large aperture[J]. *Chinese Optics*, 2014, **7**(1): 163-168.

[14] ZHU Shuo, ZHANG Xiao-hui. Application of error detaching to Ritchey-Common test for flat mirrors[J]. *Optics and Precision Engineering*, 2014, **22**(1): 7-12.

[15] YANF Fei, AN Qi-chang, ZHANG Jing-xu. Mirror surface figure evaluation based on power spectral density[J]. *Chinese Optics*, 2014, **7**(1): 156-162.

[16] XU Yang, TANG Feng, WANG Xiang-chao, *et al*. Mmeasurement error analysis of absolute flatness test[J]. *Chinese Laser*, 2011, **38**(10): 1008009.